

# Can rooted staggered fermions describe nonzero baryon density at low temperatures?

Szabolcs Borsányi<sup>1</sup>, Zoltán Fodor,<sup>1,2,3,4,5</sup> Matteo Giordano<sup>3</sup>, Jana N. Guenther,<sup>1</sup> Sándor D. Katz,<sup>3</sup>  
Attila Pásztor<sup>3,6,\*</sup> and Chik Him Wong<sup>1</sup>

<sup>1</sup>*Department of Physics, Wuppertal University, Gaußstraße 20, D-42119, Wuppertal, Germany*


<sup>2</sup>*Pennsylvania State University, Department of Physics, State College, Pennsylvania 16801, USA*

<sup>3</sup>*Institute for Theoretical Physics, ELTE Eötvös Loránd University,  
Pázmány P. sétány 1/A, H-1117 Budapest, Hungary*

<sup>4</sup>*Jülich Supercomputing Centre, Forschungszentrum Jülich, D-52425 Jülich, Germany*

<sup>5</sup>*Physics Department, UCSD, San Diego, California 92093, USA*

<sup>6</sup>*HUN-REN-ELTE Theoretical Physics Research Group,  
Pázmány Péter sétány 1/A, H-1117 Budapest, Hungary*

 (Received 13 September 2023; accepted 21 December 2023; published 25 March 2024)

Research on the quantum chromodynamics (QCD) phase diagram with lattice field theory methods is dominated by the use of rooted staggered fermions, as they are the computationally cheapest discretization available. We show that rooted staggered fermions at a nonzero baryochemical potential  $\mu_B$  predict a sharp rise in the baryon density at low temperatures and  $\mu_B \gtrsim 3m_\pi/2$ , where  $m_\pi$  is the Goldstone pion mass. We elucidate the nature of the nonanalyticity behind this sharp rise in the density by a comparison of reweighting results with a Taylor expansion of high order. While at first sight this nonanalytic behavior becomes apparent at the same position where the pion condensation transition takes place in the phase-quenched theory, the nature of the nonanalyticity in the two theories appears to be quite different: While at nonzero isospin density the data are consistent with a genuine thermodynamic (branch-point) singularity, the results at nonzero baryon density point to an essential singularity at  $\mu_B = 0$ . The effect is absent for four flavors of degenerate quarks, where rooting is not used. For the two-flavor case, we show numerical evidence that the magnitude of the effect diminishes on finer lattices. We discuss the implications of this technical complication on future studies of the QCD phase diagram.

DOI: [10.1103/PhysRevD.109.054509](https://doi.org/10.1103/PhysRevD.109.054509)

## I. INTRODUCTION

Despite decades of effort, the determination of the phase diagram of quantum chromodynamics (QCD) on the temperature ( $T$ )–baryochemical potential ( $\mu_B$ ) plane remains an unsolved problem, due to the complex action problem hampering first-principle lattice QCD calculations. Nevertheless, several workarounds have been proposed and utilized to obtain information at nonzero  $\mu_B$ , such as a Taylor expansion around  $\mu_B = 0$  [1–11], analytic continuation from imaginary chemical potentials [12–27], and different reweighting techniques [28–38].

Since all of these workarounds require very large statistics, rooted staggered fermions [39–41] are the most

popular fermion discretization in the literature for being the most computationally efficient. In fact, we are not aware of any results with physical quark masses on finite baryon density QCD from nonstaggered formulations. Similarly, continuum extrapolation at finite baryon density has only ever been attempted with rooted staggered fermions. It is unfortunate then, that the theoretical justification of the application of rooted staggered fermions at finite chemical potential is not fully settled [42,43].

For simplicity, we discuss the case when a chemical potential is only introduced for degenerate light quarks, and not for the strange quark. In this case one has to deal with complex square roots instead of fourth roots. Since the staggered determinant is complex at real chemical potential, one must find a way to resolve the sign ambiguity in the complex square root function. One possible way is to demand the determinant to be a continuous function of the chemical potential along the real axis [31]. In Ref. [42] a simple counting argument was given, that suggests that this procedure leads to cutoff effects of the order  $\mathcal{O}(a)$ , where  $a$  is the lattice spacing. The counting argument is based on the

\*Corresponding author: [apasztor@bodri.elte.hu](mailto:apasztor@bodri.elte.hu)

*Published by the American Physical Society under the terms of the Creative Commons Attribution 4.0 International license. Further distribution of this work must maintain attribution to the author(s) and the published article's title, journal citation, and DOI. Funded by SCOAP<sup>3</sup>.*

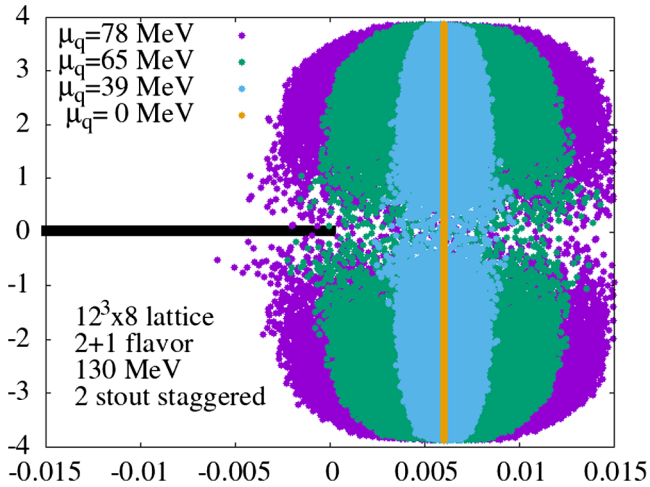


FIG. 1. Illustration of the Dirac spectrum at finite baryochemical potential. The spectrum, obtained with dense linear algebra, is based on one dynamical staggered lattice configuration of size  $12^3 \times 8$  with  $m_\pi = 135$  MeV, using the 2stout action. The thick line shows the standard choice for the branch cut of the complex square root.

observation that the taste multiplets in the Dirac spectrum are of size  $\mathcal{O}(a)$ . Unfortunately, it gives no indications about the chemical potential dependence of these cutoff effects.

Since the branch point singularities of the complex square root function are located at the zeros of its argument, the problems caused by the ambiguity in rooting are expected to be severe at values of the chemical potential near a complex zero of the (unrooted) staggered determinant. At zero temperature, this is expected to happen for light-quark chemical potentials  $\mu_q = \frac{\mu_B}{3} \gtrsim \frac{m_\pi}{2}$  [44,45]. See Fig. 1 for an illustration at a temperature in the confined phase. How thermodynamic observables are affected by these branch point singularities has, however, never been studied in detail. This is the purpose of this work.

The structure of this paper is the following: First, in Sec. II we revisit reweighting methods, including methods that are free from an overlap problem [34,35,38]. The use of such methods is important, as they allow us to safely rule out an overlap problem in our results.

In Sec. III, we show that rooted staggered fermions predict a sharp rise in the light-quark density around  $\mu_q = \mu_B/3 \gtrsim m_\pi/2$  if we resolve the rooting ambiguity by requiring that the determinant is a continuous function at real  $\mu_B \geq 0$ . This sharp rise occurs at values of the quark chemical potential where, in the phase-quenched theory, the isospin density shows a sharp rise [46]. In the latter case, which is equivalent to a theory with nonzero isospin chemical potential, the rise of the isospin density signals the condensation of pions [47,48].

At first sight, it thus appears that the baryon chemical potential ensemble has some remnant of the pion condensation transition at nonzero isospin chemical potential. In fact, this behavior was seen before in Ref. [49], where the

authors attempted to reweight ensembles generated at a nonzero isospin chemical potential to a nonzero baryochemical potential. At that point in time, however, it could not be determined whether the cause of this issue was an overlap problem from reweighting or a problem with staggered rooting. With the methods discussed in Sec. II, we can now safely rule out an overlap problem.

To confirm that the cause of the issue is indeed rooting, we show results from simulations with four flavors of degenerate quarks in Sec. IV. When the chemical potential is nonzero for only two of the four flavors (which requires rooting), the rapid rise of the density at half the pion mass is again present. On the other hand, if the chemical potential is the same for all four flavors (which requires no rooting), the issue is not observed. Admittedly, the error bars on the  $N_f = 4$  data are substantially larger, due to a stronger sign problem in that case.

The question then remains: To what extent can the observed increase in the density at nonzero  $\mu_B$  be considered a remnant of the pion condensation transition? To make the question more concrete: is the analytic structure of the free energy at nonzero  $\mu_B$  similar to what one expects for a thermodynamic transition, or is there any difference? In Sec. V, we elucidate the nature of the nonanalyticity introduced by staggered rooting by comparing results from reweighting methods to results obtained by performing a Taylor expansion of the partition function at zero chemical potential, which we calculated to unprecedentedly high orders. At low temperature, in spite of the Taylor coefficients computed at zero chemical potential being exactly the same as the Taylor coefficients of the expansion of the reweighted pressure, the two methods appear to converge to different curves. This suggests that the rooted staggered free energy is nonanalytic in the chemical potential, with a nonanalytic term having an identically zero Taylor expansion. Such a behavior is not expected around zero on thermodynamical grounds, since the QCD transition for vanishing baryon density is a crossover. This behavior is also very different from the nonanalytic behavior at a typical thermodynamic transition or crossover: Even though these are also characterized by a sudden rise in the density as a function of the chemical potential, the behavior of the Taylor series is very different. For a phase transition or a crossover, the Taylor expansion should diverge near the transition point [50]. We also demonstrate this contrasting behavior using lattice data by comparing a high order Taylor expansion with reweighting at a nonzero isospin density.

Next, in Sec. VI, we numerically extract the nonanalytic part (under some assumptions) for a discretization with strongly suppressed taste breaking—known as 4HEX improved staggered fermions [51]—for three different lattice spacings ( $N_\tau = 6, 8, 10$ ) and observe a strong decrease in the magnitude of the nonanalytic part, which is an indication that this sharp rise in the density for  $\mu_B \gtrsim 3m_\pi/2$  is a cutoff effect.

In the final section we summarize our results and discuss several strategies which future simulation projects can use to overcome this roadblock introduced by staggered rooting.

## II. ROOTED STAGGERED QUARKS AT FINITE $\mu_B$

The dimensionless pressure is related to the grand canonical partition function  $\mathcal{Z}$  of a thermodynamic system via:

$$\hat{p} \equiv \frac{P}{T^4} = \frac{1}{T^3 V} \log \mathcal{Z}, \quad (1)$$

where  $T$  is the temperature and  $V$  is the spatial volume. In this paper we deal with the grand canonical partition functions of QCD and related models at finite quark chemical potential, studying in particular the chemical potential dependence of the quark density-to-chemical potential ratio, defined as:

$$\frac{\hat{n}_L}{\hat{\mu}_q} \equiv \frac{1}{\hat{\mu}_q} \frac{\partial \hat{p}}{\partial \hat{\mu}_q} = \frac{1}{\mu_q T V} \frac{\partial \log \mathcal{Z}}{\partial \mu_q}, \quad (2)$$

where  $\hat{n}_L = n_L/T^3$  and  $\hat{\mu}_q = \mu_q/T$ . We will apply Eqs. (1) and (2) for different theories, with different flavor content and choices for the chemical potentials throughout this manuscript.

For the case of  $N_f = 2 + 1$  flavors of rooted staggered fermions, the grand canonical partition function reads schematically:

$$\mathcal{Z}_{2+1}(T, \mu_q) = \int \mathcal{D}U \det M^{1/2}(U, m_u, \mu_q) \times \det M^{1/4}(U, m_s, 0) e^{-S_{\text{YM}}(U)}. \quad (3)$$

Here  $M$  is the massive staggered operator,  $m_u$  and  $m_s$  are the light- and strange quark masses, respectively,  $\mu_q$  is the chemical potential of the light quarks, while we set the strange quark chemical potential  $\mu_s = 0$ , which is the setup we use throughout the paper. Moreover,  $S_{\text{YM}}$  is the discretized Yang-Mills action and  $U$  are the link variables.

Since the integrand in Eq. (3) is complex, the partition function at finite chemical potential cannot be numerically simulated using standard importance-sampling methods. In this paper we side-step this problem using reweighting techniques, i.e., performing a numerical simulation using importance sampling of a related theory free from the complex-action problem, and then suitably rescaling the weight of each configuration so that it matches the (complex) one found in the target theory. We will obtain the same result with three different reweighting schemes, which we describe in the following:

### A. Reweighting from $\mu_B = 0$

In what is arguably the simplest reweighting technique, one generates configurations at  $\mu_q = 0$  and calculates the partition function, its logarithm and the derivatives of its logarithm by starting with the formula:

$$\frac{\mathcal{Z}_{2+1}(\mu_q)}{\mathcal{Z}_{2+1}(\mu_q = 0)} = \left\langle \frac{\det M^{1/2}(U, m_u, \mu_q)}{\det M^{1/2}(U, m_u, 0)} \right\rangle_{\mu_q=0}, \quad (4)$$

where  $\langle \dots \rangle_{\mu_q=0}$  denotes expectation values calculated at  $\mu_q = 0$ . Derivatives of the pressure follow by simply differentiating the natural logarithm of Eq. (4).

The ratio of determinants in Eq. (4) can be conveniently calculated using the reduced matrix formalism [52]. The staggered reduced matrix is a complex matrix of size  $6N_s^3 \times 6N_s^3$ , where  $N_s^3$  is the spatial lattice volume in lattice units. The reduced matrix is a function of the gauge links as well as the quark mass, but, most importantly, it is independent of the chemical potential. Using the notations of Ref. [43] one can express the staggered determinant of the four-flavor theory for a given configuration ( $U$ ) at any quark chemical potential ( $\mu_q$ ) using only the eigenvalues ( $\xi_i$ ) of the reduced matrix as

$$\frac{\det M(U, m, \mu_q)}{\det M(U, m, 0)} = e^{-3N_s^3 \mu_q/T} \prod_{i=1}^{6N_s^3} \frac{\xi_i[m, U] - e^{\mu_q/T}}{\xi_i[m, U] - 1}. \quad (5)$$

The *complex eigenvalues* ( $\xi_i$ ) can be computed using dense linear algebra packages [53].

The rooting procedure for a complex fermion determinant is inherently ambiguous, and the ratio of rooted determinants in Eq. (4) is not well defined until this ambiguity is resolved. A reasonable choice is to compute this ratio by taking the square root of Eq. (5) eigenvalue by eigenvalue [30,43]:

$$\frac{\det M^{1/2}(U, m, \mu_q)}{\det M^{1/2}(U, m, 0)} := e^{-3N_s^3 \mu_q/T} \prod_{i=1}^{6N_s^3} \sqrt{\frac{\xi_i[m, U] - e^{\mu_q/T}}{\xi_i[m, U] - 1}}. \quad (6)$$

The branch cut of the complex square root on the right hand side is put on the negative real axis. Notice that none of the fractions under the square roots will ever cross the branch cut of the square root function as long as  $\mu_q$  is real. As a consequence, the rooted determinant as defined in Eq. (6) continuously connects to the positive real root of the determinant at  $\mu_q = 0$  starting from any real value of  $\mu_q = \mu_B/3$ .

While Eq. (4) is exact for infinite statistics, the probability distribution of the weights  $\frac{\det^{1/2} M(U, m_u, \mu_q)}{\det^{1/2} M(U, m_u, 0)}$  can be heavy tailed, and thus hard to sample (an overlap problem). It is therefore hard to judge the reliability of this reweighting approach on its own, without also using other

techniques. To cross-check the reweighting method from  $\mu_q = 0$  we utilize two other reweighting schemes for which the weights take values from a compact domain. By construction, probability distributions with a compact support have no tails, and therefore no overlap problem.

### B. Phase reweighting

For this reweighting scheme, the simulated ensemble is the phase-quenched ensemble, with quark determinant replaced by its absolute value. The partition function of the phase-quenched ensemble reads:

$$\mathcal{Z}_{2+1}^{\text{PQ}}(T, \mu_q) = \int \mathcal{D}U |\det M^{1/2}(U, m_u, \mu_q)| \times \det M^{1/4}(U, m_s, 0) e^{-S_{\text{YM}}(U)}, \quad (7)$$

and is identical to the partition function with a finite isospin chemical potential, with  $\mu_q = \mu_u = -\mu_d$ . The partition function at finite baryochemical potential is obtained from the phase-quenched ensemble as

$$\frac{\mathcal{Z}_{2+1}}{\mathcal{Z}_{2+1}^{\text{PQ}}} = \left\langle \frac{\det M^{1/2}(U, m_u, \mu_q)}{|\det M^{1/2}(U, m_u, \mu_q)|} \right\rangle_{\text{PQ}}, \quad (8)$$

where  $\langle \dots \rangle_{\text{PQ}}$  denotes the expectation value in the phase-quenched theory, defined by Eq. (7). The weights in this case are pure phases, i.e., the reweighting factors are elements of the unit circle, which form a compact domain, on which no long-tailed distributions are possible.

While the idea of phase reweighting has been around for decades, the first simulations in the actual phase-quenched ensemble have been carried out only two years ago [35]. Previous studies always included an explicit symmetry-breaking term [54], usually denoted  $\lambda$ , which amounts to the substitution  $|\det M|^{1/2} \rightarrow \det(M^\dagger M + \lambda^2)^{1/4}$  in Eq. (7). In the  $\lambda \rightarrow 0$  limit this formulation allows theoretically clean investigations of pion condensation, making it a preferable choice for nonzero isospin density. However, when simulations are performed with the intent to subsequently reweight to nonzero  $\mu_B$ , the  $\lambda$  term is not desirable, as it leads to an overlap problem in the  $\lambda \rightarrow 0$  reweighting step. How simulations at  $\lambda = 0$  are performed is explained in Ref. [35].

### C. Sign reweighting

Here the partition function is defined as:

$$\mathcal{Z}_{2+1}^{\text{SQ}}(T, \mu_q) = \int \mathcal{D}U |\text{Re det } M^{1/2}(U, m_u, \mu_q)| \times \det M^{1/4}(U, m_s, 0) e^{-S_{\text{YM}}(U)}, \quad (9)$$

and the ratio of the desired finite baryon density vs the sign-quenched partition function is

$$\frac{\mathcal{Z}_{2+1}}{\mathcal{Z}_{2+1}^{\text{SQ}}} = \left\langle \frac{\text{Re det } M^{1/2}(U, m_u, \mu_q)}{|\text{Re det } M^{1/2}(U, m_u, \mu_q)|} \right\rangle_{\text{SQ}}, \quad (10)$$

where  $\langle \dots \rangle_{\text{SQ}}$  denotes the expectation value in the sign-quenched theory, defined by Eq. (9). The reweighting factors can only take two values: +1 or -1. Hence the distribution of the weights is a one parameter probability distribution (the Bernoulli distribution). Again, by construction, there are no tails and thus no overlap problem. Note that the substitution of the quark determinant to its real part is not allowed in generic expectation values, as the path integral representation of expectation value will in general involve the determinant itself. The substitution is allowed, however, for the class of observables we consider here: i.e., observables that can be defined as real derivatives of the partition function with respect to real parameters, like the quark mass or the chemical potential.

### III. A RISE IN THE DENSITY AT $\mu_B \gtrsim 3m_\pi/2$

We have recently shown that for the equation of state of the quark gluon plasma in the range  $\mu_B/T \leq 3$ , reweighting gives compatible results with analytic continuation from purely imaginary chemical potentials [38]. Thus, in the currently experimentally accessible range (the range of the RHIC Beam Energy Scan, phase two) the equation of state of the quark-gluon plasma is under control. In particular, the resummations introduced in Refs. [55,56], an 8th-order Taylor expansion and the overlap problem free reweighting techniques of Refs. [34,35] agree in this range for  $\frac{\mu_B}{\mu_q}$ . The lowest temperature studied in Ref. [38] was 145 MeV.

When attempting to extend these reweighting studies to lower temperatures, we have noticed a sharp rise in the density as a function of the chemical potential at around  $\mu_B = 3m_\pi/2$ . This is shown for a temperature of  $T = 130$  MeV in Fig. 2. Results in this plot were obtained with a lattice size of  $16^3 \times 8$ . We use physical quark masses, using a tree-level improved gauge action and 2 steps of stout smearing [57] with smearing parameter  $\rho = 0.15$  applied to the links entering the staggered Dirac operator, which we will call the 2stout action [58,59] from now on. To better see the onset of this sharp increase, we also show the 8th-order Taylor expansion, as a smooth baseline. Note that in this work we compute Taylor expansions around  $\mu_q = 0$  using the reduced matrix formalism [52], without employing stochastic estimators.

This sharp rise in the density is very similar to the way the isospin density behaves at the pion condensation transition [46], a transition that happens in the phase-quenched theory around the same value  $\mu_q = m_\pi/2$  of the quark chemical potential. In fact, it was seen before in the literature that at  $\mu_B = 3m_\pi/2$ , something that looks similar to a phase transition takes place. This was observed when attempting to reweight to a nonzero baryochemical potential from a nonzero isospin chemical potential in Ref. [49].

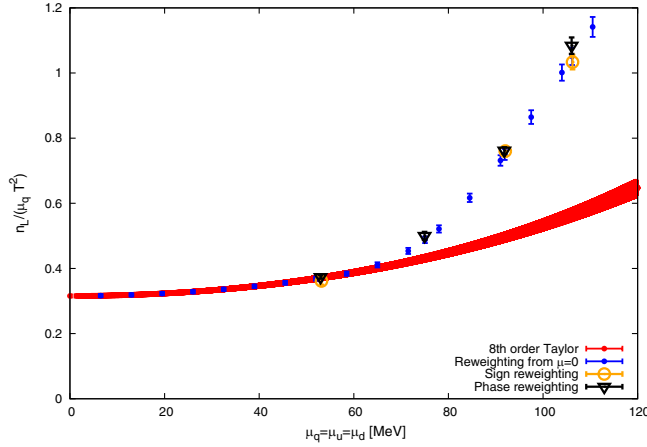


FIG. 2. A rapid rise in the light-quark density-to-chemical potential ratio as a function of  $\mu_q$  around  $\mu_q = m_\pi/2$  with rooted staggered fermions. We used the 2stout improved action, with a lattice size of  $16^3 \times 8$  and a temperature of  $T = 130$  MeV. To lead the eye and see where the increase sets in, an 8th-order Taylor expansion is also shown. Reweighting from  $\mu_q = 0$ , phase reweighting, and sign reweighting (see Sec. III) all give the same result, indicating a lack of an overlap problem.

The main difference between that work and ours is that we did not introduce an infrared regulator that lifts the mass of the Goldstone boson that emerges as a result of the symmetry-breaking transition. We avoided using this regulator to guard our simulations from an additional overlap problem.

The strong deviation of the reweighted results from the Taylor expansion in Fig. 2 prompts for cross-checks. Indeed, we computed the sharp rising baryon density using the three different reweighting schemes discussed in the previous section, all giving the same result, and ruling out an overlap problem. Since we have established the reliability of these schemes, we will exclusively use reweighting from

$\mu_q = 0$  in the further sections of the paper, to keep the computer time budget manageable.

#### IV. THE FOUR-FLAVOR THEORY

If the observed sharp rise in the quark density is due to staggered rooting, it should be absent in the four-flavor theory, where rooting is absent and the partition function with staggered fermions is given by

$$\mathcal{Z}_4(T, \mu_q) = \int \mathcal{D}U \det M(U, m, \mu_q) e^{-S_{\text{YM}}(U)}, \quad (11)$$

where  $m$  is the quark mass for all four flavors. We can calculate expectation values of observables in this theory by reweighting from zero chemical potential, similarly to the  $2 + 1$  flavor case.

On the other hand, the sharp rise in the density should be observed if we only introduce a chemical potential for only two of the four flavors:

$$\mathcal{Z}_{2+2}(T, \mu_q) = \int \mathcal{D}U \det M^{1/2}(U, m, \mu_q) \times \det M^{1/2}(U, m, 0) e^{-S_{\text{YM}}(U)}. \quad (12)$$

We have performed simulation at  $\mu_q = 0$  for the four-flavor theory, with quark masses corresponding to a pion mass of  $m_\pi = 260$  MeV [60], a temperature  $T = 100$  MeV and a lattice volume of  $12^3 \times 8$ . The scale was set using the  $w_0$  scale of Ref. [66]. We calculated the eigenvalues of the reduced matrix for 0.9 million configurations. With this pion mass the inflection point of the renormalized chiral condensate gives a cross-over temperature of approximately 135 MeV. We then proceeded to calculate the ratio  $\hat{n}_L/\hat{\mu}_q$  for both assignments of the chemical potentials, i.e., when all four quarks get the same chemical potential vs when only

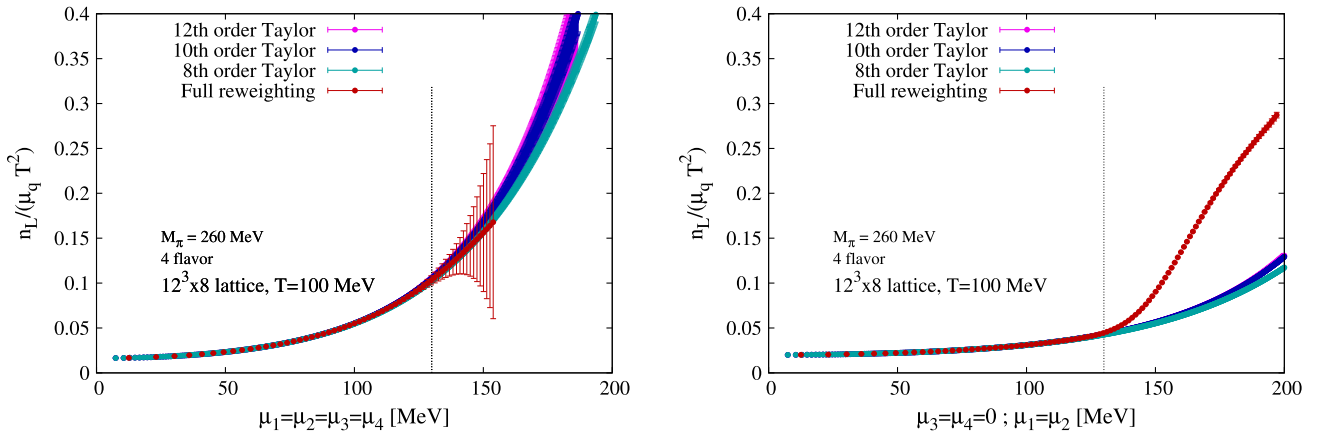


FIG. 3. The density to chemical potential ratio for four flavors of quarks. Left: all quarks having the same chemical potential (this choice requires no rooting). Right: the chemical potential is introduced only for two of the four flavors, while the other two flavors remain at zero chemical potential (this choice requires rooting). Both cases were calculated using the same  $\mu_q = 0$  ensemble. The vertical line corresponds to  $\mu_q = m_\pi/2$ .

two of them do. The results can be seen in Fig. 3. While the four-flavor case  $\mu_1 = \mu_2 = \mu_3 = \mu_4 = \mu_q$  becomes quite noisy at large  $\mu_q$ , the difference between the two cases is rather clear to see. In the four-flavor case the Taylor expansion and the full reweighting match within errors. In the case of  $\mu_1 = \mu_2 = \mu_q$  with  $\mu_3 = \mu_4 = 0$ , the reweighted curve rises sharply near  $\mu_q = m_\pi/2$ , and there is a very clear deviation between the Taylor and reweighted curves. This resembles the sharp rise in the quark density that we observed in the 2 + 1-flavor case. The statistical errors for the (unrooted) four-flavor case are admittedly large at large  $\mu_q$ . The error grows large precisely at the chemical potential where the rooted case takes a sharp turn, indicating large cancellations.

To understand why the errorbars for  $N_f = 4$  are so large, we note that the leading order formula for the exponential severity of the sign problem has a factor of  $N_f^2$  in the exponent [35]:

$$\langle e^{i\theta} \rangle_{\text{PQ}}^{\text{LO}} = \exp\left(-\frac{N_f^2}{18} \chi_{11}^{ud} (\text{LT})^3 \left(\frac{\mu_B}{T}\right)^2\right), \quad (13)$$

where  $\chi_{11}^{ud} = \frac{1}{T^2} \left(\frac{\partial^2 p}{\partial \mu_u \partial \mu_d}\right)_{\mu_u = \mu_d = 0}$  is the disconnected part of the light quark susceptibility. This leads to the expectation of a much more severe sign problem in the four-flavor theory than in the two-flavor theory. In Fig. 4 we show the leading order estimate of the severity of the sign problem as a function of  $2\mu_q/m_\pi$  for  $N_f = 4$ , as well as the full measured sign problem for  $N_f = 4$ , and the fourth power of the measured sign problem for the case when we only introduce a chemical potential for two flavors. What we see is that while the leading order formula is no longer accurate

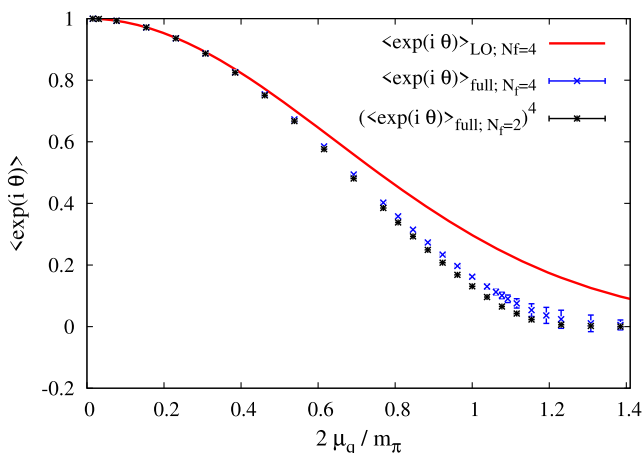


FIG. 4. The expectation value of the phases for  $N_f = 4$  from the leading order formula in Eq. (13) (red line) and from the actual simulations (blue data points) as well as the expectation value for the case when the chemical potential is only introduced for two flavors, but taken to the 4th power (black data points).

above  $\mu_q \approx m_\pi/2$ , the  $N_f^2$  scaling of severity of the sign problem still holds—at least to a good approximation—for larger  $\mu_q$ . This scaling of the sign problem cannot be easily converted to the error bars on the density, since in addition to the phases, the probability distribution of the observables as well as the correlations between the observable and the phases also matters. But it does explain that error bars for the four-flavor case should be considerably larger.

In summary, our findings are in line with our assumption that the sharp rise in the light-quark density for  $\mu_B \gtrsim 3m_\pi/2$  is caused by staggered rooting.

## V. ANALYTIC STRUCTURE AND PION MASS DEPENDENCE

Next, we try to answer the question: to what extent is this sharp rise in the quark density in the nonzero baryochemical potential ensemble similar to or different from the sharp rise in the isospin density in the nonzero isospin ensemble. More precisely: Is the complex singularity behind these two behaviors of the same type?

In order to clarify the analytic structure behind the observed rise in the density, we have performed high statistics simulations on  $12^3 \times 8$  lattices with the 2stout action at physical quark masses, and measured Taylor coefficients of the pressure to 12th order in the chemical potential both for physical quark masses and also for four times the physical value of the quark masses (which correspond to twice the physical pion mass to leading order in chiral perturbation theory). When converting results to MeV in the heavy-pion case, we assumed that the lattice scale does not change when changing the light quark mass. This assumption is approximately correct as the scale depends more strongly on the mass of the strange quark. Our results can be seen in the left panel of Fig. 5.

For comparison, we also show the Taylor expansion and the full reweighting for the case of an isospin chemical potential (with no explicit symmetry breaking parameter) in the right panel of Fig. 5. For the case of an isospin chemical potential the rapid rise in the density is due to a second order phase transition [47,48] at  $\mu_q \approx m_\pi/2$ . In such a case the free energy is analytic at  $\mu_q = 0$  and has a branch-point singularity at the nearest Lee-Yang zero [10,67–69], limiting the radius of convergence. At large enough orders in the finite-volume Taylor expansion a crossover, a second order transition and a first order transition are not that different, as the position of a Lee-Yang zero must have a nonzero imaginary part  $\Delta_{\text{LY}}$ , which for a true phase transition vanishes in the thermodynamic limit, while for a crossover remains finite. In this situation the radius of convergence in a finite volume is given approximately by  $R \approx \sqrt{\mu_c^2 + \Delta_{\text{LY}}^2}$ , where  $\mu_c$  is the chemical potential of the transition in the infinite-volume limit. For large enough orders, the nonzero  $\Delta_{\text{LY}}$  leads to a complicated sign structure for the high order coefficients [10]. We do not observe this up to 12th order in

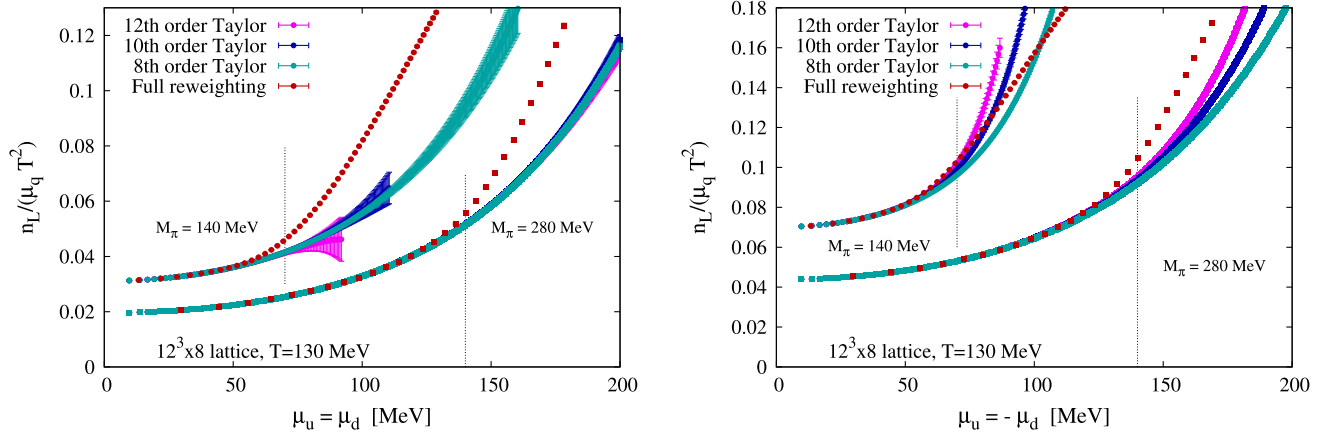


FIG. 5. The full reweighted results for the light-quark density compared with several high orders of the Taylor expansion for the case of a baryon (left panel) and isospin (right panel) chemical potential for two different values of the pion mass. While the density itself looks very similar in the two cases, with a rapid rise for  $\mu_q \gtrsim m_\pi/2$ , the two singularities appear to be very different: At a finite isospin chemical potential—where the singularity of the free energy is due to a true phase transition—the Taylor expansion converges to the full reweighting result below  $\mu_q \approx m_\pi/2$ , and diverges above. On the other hand, at a finite baryon chemical potential, the Taylor expansion appears to converge, but above  $\mu_q \approx m_\pi/2$  it converges to a different curve than the full reweighting one. This hints at a very different analytic structure.

the Taylor expansion, however. Rather, at finite isospin chemical potential all Taylor coefficients up to this order are positive, and the radius of convergence can be estimated with a simple ratio estimator to be close to the expected  $R \approx m_\pi/2$ . Thus the Taylor expansion should converge to the full result until the transition point, above which it should diverge. This is exactly what is seen in the right panel of Fig. 5, at both of the simulated pion masses. The one important difference is that for the larger pion mass, the Taylor expansion seems to converge more slowly. This is not surprising, as the expansion parameter is  $\mu_q/T$ , which is larger at the transition point for a heavier pion.

Such divergent behavior is typical for phase transitions. It is very different from the behavior we observe at nonzero baryon density, seen in the left panel of Fig. 5. Here, the Taylor expansion appears to converge, but it converges to a different curve from the one obtained with full reweighting. Let us emphasize that the Taylor coefficients and the reweighting curve were obtained using the same gauge ensembles, and so the Taylor coefficients are exactly the Taylor coefficients of the reweighted curve at  $\mu_q = 0$ . Also note that while the point of divergence between the reweighting and Taylor curves does seem to scale with the pion mass, the two curves actually start to diverge already somewhat below  $\mu_q = m_\pi/2$ . This points to quite different nonanalytic behavior, compared to the case of a nonzero isospin density. One example of a nonanalytic term in the free energy which could produce such a behavior is

$$A\mu_q^\alpha e^{-\frac{\Lambda^2}{\mu_q^2}}, \quad (14)$$

where  $A$ ,  $\alpha$  and  $\Lambda$  are parameters. A term of this form in the free energy would not affect the Taylor expansion at all, but it would lead to a sharp increase in the density at some value of  $\mu \approx \Lambda$ . If  $\Lambda$  also scaled with the pion mass, then so would the value at which the sharp increase appears. If such terms are indeed the cause of the sharp rise of the light-quark density, then the nonanalyticity of the free energy with rooted staggered fermions would actually be located at  $\mu_q = 0$  and not near  $\mu_q = m_\pi/2$ .

While it is impossible to prove that the free energy has a term of this form by using only numerical simulations, there are two pieces of evidence that support this conjecture.

First, one can easily construct two particular schemes of the complex rooting that differ in the free energy in the conjectured form.

- (i) Consider Eq. (6), which is designed to be continuous in real  $\mu_q$  and has been used, e.g., in Fig. 5 for the “full reweighting” data.
- (ii) Consider the square root of the determinant where we always take the root with a positive real part.

Notice that the second definition will never lead to a sign problem. In fact, the second definition gives the sign-quenched partition function [see Eq. (9)] of the first definition. One can show (see the Appendix of Ref. [35]) that the difference between the two free energies is of the conjectured form, with  $\alpha = 3$ ,

$$f - f_{\text{SQ}} \sim A\mu_q^3 e^{-B/\mu_q^2}. \quad (15)$$

Thus, the Taylor series of (i) and (ii) schemes are identical and the two free-energies near  $\mu_q = 0$  differ in a function with an essential singularity. One therefore expects that

different choices of the rooting procedure lead to different singularities. However, we are not aware of any choice where analyticity at  $\mu_q = 0$  is guaranteed.

Second, the conjectured form of the nonanalytic part fits the lattice simulation data well. Thus, while the exact functional form is hard to determine from numerical data alone, the numerical evidence points to the rooted staggered free energy having an essential singularity at  $\mu_q = 0$ .

Finally, we point out that an essential singularity of the form shown in Eq. (14) is (strictly speaking) only possible for infinite statistics. For any finite statistics, the leading singularity in the free energy should be the branch-point singularity given by the closest of the determinant zeros [complex logarithms of the  $\xi_i$  eigenvalues of the reduced matrix in Eq. (5)] in the ensemble. In the limit of infinite statistics the branch-points could get arbitrarily close to  $\mu_q = 0$ . Then the accumulation of these branch-point singularities could produce an essential singularity. Strictly speaking this means that at finite statistics, the Taylor series has a finite radius of convergence, given by the closest branch-point singularity, while in the limit of infinite statistics, the radius of convergence tends to zero, in the sense of an essential singularity at  $\mu_q = 0$ . Only in the limit of infinite statistics, is the Taylor expansion oblivious to the branch points. We have seen such behavior while accumulating the statistics for Fig. 5. When we had only around 100 000 configurations, the Taylor coefficients  $\chi_{10}^L$  and  $\chi_{12}^L$  looked like they had a nonzero value within errors, and estimators of the radius of convergence gave results between 60 and 70 MeV. After doubling the statistics, the signal for  $\chi_{10}^L$  and  $\chi_{12}^L$  disappeared, and behavior similar to the one shown in the left panel of Fig. 5 emerged, which then remained stable after doubling the statistics two more times. Thus, the estimators of the radius of convergence with the smaller statistics were most likely dominated by a few configurations with close-by branch point singularities, and only after substantially increasing the statistics did the behavior become apparently consistent with an essential singularity.

## VI. CONTINUUM SCALING WITH AN ACTION WITH STRONGLY SUPPRESSED TASTE BREAKING

A natural question that arises is whether the observed nonanalytic behavior of the free energy of rooted staggered fermions vanishes in the continuum limit, or not. To study this question, we used a discretization with strongly suppressed taste breaking: the DBW2 gauge action [70–72] and 4 steps of hex smearing [73], which we will call the 4HEX action [51]. For this simulation we used physical quark masses [51] at temperature  $T = 130$  MeV, aspect ratio  $LT = 2$ , and three different lattice spacings corresponding to  $N_\tau = 6, 8$  and 10 time-slices each. In Fig. 6 we show the difference between full reweighting and an 8th-order Taylor

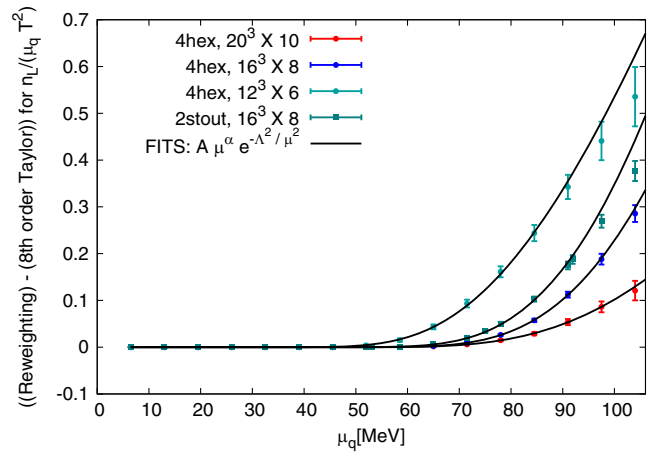


FIG. 6. The difference between the full reweighted result and the 8th-order Taylor expansion (which is assumed to be a good proxy for the analytic part of the density) for the light-quark density in units of the dimensionless quark chemical potential for the 4HEX action with 6, 8 and 10 timeslices respectively. For comparison, results with the 2stout action with 8 timeslices are also shown. We also show fits of the form  $A\mu_q^\alpha e^{-\Lambda^2/\mu_q^2}$ . The fits were performed in the chemical potential range up to 85 MeV.

expansion for the ratio  $\hat{n}_L/\hat{\mu}$ . For comparison, we also show results with the 2stout action at  $N_\tau = 8$ . One can see that the magnitude of the difference decreases rapidly with the lattice spacing. We did not manage to find a good fit ansatz to extrapolate this difference to the continuum, however. In particular, we do not observe the  $\mathcal{O}(a)$  scaling which is the expectation from the naive counting argument given in [42]. This might be due to the coarsest lattice ( $N_\tau = 6$ ) being too coarse for seeing the asymptotic behavior. Notice, however, that if one assumes that the difference extrapolates to zero, then the observed decrease is not slower than the expected  $\mathcal{O}(a)$ , but faster: rescaling the  $N_\tau = 8$  data by a factor of  $8/10$  gives numbers that are significantly above the lattice data at  $N_\tau = 10$ . Even rescaling the  $N_\tau = 8$  data by  $(8/10)^2$ , the data on the  $N_\tau = 10$  lattices is significantly below. Comparison with the 2stout results shows that at the same number of timeslices, the 4HEX action has a smaller nonanalytic term. This is consistent with the expectation that reduced taste breaking (and thus the splitting of the taste multiplets in the spectrum) reduces this nonphysical effect in the quark density.

## VII. SUMMARY AND DISCUSSION

We have shown that the free energy of QCD at nonzero baryochemical potential with rooted staggered fermions (with the rooting ambiguity resolved by requiring continuity for real values of the chemical potential configuration by configuration) has a nonanalytic term, that manifests itself as a rapid rise of the light-quark density at low temperatures and baryochemical potential  $\mu_B = 3\mu_q \gtrsim 3m_\pi/2$ . This is at the same values of the quark chemical potential  $\mu_q$  where



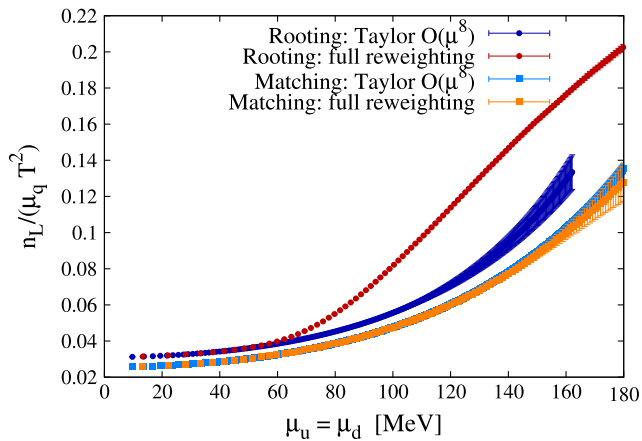


FIG. 7. Geometric matching vs standard rooting on the  $12^3 \times 8$  2stout ensemble at a temperature  $T = 130$  MeV. We show both full reweighting and Taylor expansion results. The sharp rise around  $\mu_q = m_\pi/2$  is not observed with the geometric matching procedure.

the phase-quenched ensemble has a pion condensation transition. We showed that the nonanalyticity is very different from a true thermodynamic phase transition by comparing with the case of an isospin chemical potential. Although the behavior of the light-quark density as a function of the chemical potential looks very similar in the two cases, the phase transition at nonzero isospin density leads to a branch-point singularity at some nonzero  $\mu$ , while rooting leads to an essential singularity at  $\mu_B = 0$ .

How then can we proceed with the exploration of the QCD phase diagram at  $\mu_B > 0$ ?

The Taylor coefficients themselves can be interpreted as derivatives of the free energy with respect to an imaginary chemical potential, and thus can be defined without any ambiguous complex rooting. These can form a basis for an analytical continuation to nonzero  $\mu_B$ . However, the Taylor expansion does not define the theory nonperturbatively in  $\mu_B$ .

We have seen that the magnitude of the nonanalytic part of the free energy decreases with decreasing lattice spacings. With fine enough staggered lattices one could attempt a continuum extrapolation, which could be free from this (presumably) unphysical nonanalyticity. The use of very fine staggered lattices is, however, beyond feasibility today, especially if all eigenvalues of the reduced matrix are required to calculate the quark determinant.

An alternative approach, still within the framework of staggered fermions, is offered by Ref. [43]. One can match and pair the eigenvalues of the reduced matrix based on a geometric principle and replace such pairs with a single eigenvalue, thus halving their number. Since in the reduced matrix formalism the chemical potential is introduced after the eigenvalues of the reduced matrix have been computed, one can loosely describe this method as a way to do the rooting before introducing the chemical potential, rather

than after. In this definition of the determinant at nonzero  $\mu_q$ , nonanalytic terms of the type we empirically observed with standard rooting are explicitly forbidden, as the free energy can be shown to be analytic at  $\mu_B = 0$  [43]. We demonstrate this in Fig. 7, where we show the full reweighting and Taylor expansion results for the geometrically matched definition of the determinant. We observe good agreement between the two procedures, and no rapid rise in the light-quark density at  $\mu_B \gtrsim 3m_\pi/2$ . This is in contrast to standard rooting which is also shown in Fig. 7. (Note that the rooted and geometrically matched results were obtained using the same gauge ensemble.) While one naively expects standard rooting and geometric matching to give the same continuum limit, the confirmation of this expectation requires further research.

Note, however, that the geometric matching definition of the determinant is still unlike a true two-flavor formulation, as analyticity is guaranteed only in the chemical potential and not in the gauge fields. In particular, while the eigenvalues of the reduced matrix are smooth functions of the gauge fields, a small change in the gauge fields can change which pairs are identified in the spectrum of the reduced matrix, leading to nonanalyticity in the link variables. This is similar to standard rooting, which is also not analytic in the fields, as changing the gauge fields can lead to crossing branch cuts. In both cases, this could randomize the phases of the quark determinant. For completely random phases, uncorrelated with the observable of interest, one should simply get phase-quenched physics:

$$\langle O \rangle = \frac{\langle O e^{i\theta} \rangle_{\text{PQ}}}{\langle e^{i\theta} \rangle_{\text{PQ}}} \underset{\text{uncorr}}{\approx} \frac{\langle O \rangle_{\text{PQ}} \langle e^{i\theta} \rangle_{\text{PQ}}}{\langle e^{i\theta} \rangle_{\text{PQ}}} = \langle O \rangle_{\text{PQ}}. \quad (16)$$

Even in less extreme cases, one still expects cutoff effects with staggered fermions to be in the direction that the ensemble at nonzero baryon density is closer to the phase quenched ensemble than it should be in the continuum. This is a separate issue from analyticity in the chemical potential, and should also be present with the matching definition. Indeed, for unimproved (and unsmear) staggered fermions, reweighting results with rooting and geometric matching tend to be very close to each other [34,74].

Finally, the most obvious move in light of the observed nonanalytical feature of the rooted staggered result is to completely abandon the staggered formulation. Wilson-type fermions offer single-flavor discretizations for fermions that can be essential to define the quark determinants in settings where nonzero baryon and isospin chemical potentials are needed simultaneously, like, e.g., in the core of neutron stars. However, the explicitly broken chiral symmetry makes the Wilson formulation less desirable in the vicinity of the chiral transition and in the search of the critical endpoint in the  $T - \mu_B$  phase diagram. Recently, there is renewed interest in flavor formulations with a  $U(1)$  remnant of chiral symmetry, aka minimally doubled fermions.

As long as the two light flavors are degenerate this setup can be used to define a rooting-free quark determinant at finite  $\mu_B$ . For thermodynamic studies, the Karsten-Wilczek formulation [75,76] is a natural choice. Its anisotropy is not a fundamental obstacle in thermodynamics where the temporal direction is already special. Its renormalization beyond the one loop level [77–79] is subject to active research.

### ACKNOWLEDGMENTS

The project was supported by the BMBF Grant No. 05P21PXFCA. This work is also supported by the MKW NRW under the funding code NW21-024-A. Further funding was received from the DFG under the Project

No. 496127839. This work was also supported by the Hungarian National Research, Development and Innovation Office, NKFIH Grant No. KKP126769. This work was also supported by the NKFIH excellence Grant No. TKP2021\_NKTA\_64. The authors gratefully acknowledge the Gauss Centre for Supercomputing e.V. ([80]) for funding this project by providing computing time on the GCS Supercomputers Jureca/Juwels [81] at Juelich Supercomputer Centre, HAWK at Höchstleistungsrechenzentrum Stuttgart, and SuperMUC at Leibniz Supercomputing Centre. This research was supported by the Hungarian National Research, Development, and Innovation Fund under Project No. FK147164.

- 
- [1] Rajiv V. Gavai and Sourendu Gupta, Pressure and nonlinear susceptibilities in QCD at finite chemical potentials, *Phys. Rev. D* **68**, 034506 (2003).
- [2] C. R. Allton, M. Doring, S. Ejiri, S. J. Hands, O. Kaczmarek, F. Karsch, E. Laermann, and K. Redlich, Thermodynamics of two flavor QCD to sixth order in quark chemical potential, *Phys. Rev. D* **71**, 054508 (2005).
- [3] S. Basak *et al.*, QCD equation of state at nonzero chemical potential, *Proc. Sci. LATTICE2008* (2008) 171.
- [4] Szabolcs Borsányi, Zoltán Fodor, Sándor D. Katz, Stefan Krieg, Claudia Ratti, and Kálmán Szabó, Fluctuations of conserved charges at finite temperature from lattice QCD, *J. High Energy Phys.* **01** (2012) 138.
- [5] Sz. Borsányi, G. Endrődi, Z. Fodor, S. D. Katz, S. Krieg, C. Ratti, and K. K. Szabó, QCD equation of state at nonzero chemical potential: Continuum results with physical quark masses at order  $\mu^2$ , *J. High Energy Phys.* **08** (2012) 053.
- [6] R. Bellwied, S. Borsányi, Z. Fodor, S. D. Katz, A. Pásztor, C. Ratti, and K. K. Szabó, Fluctuations and correlations in high temperature QCD, *Phys. Rev. D* **92**, 114505 (2015).
- [7] H. T. Ding, Swagato Mukherjee, H. Ohno, P. Petreczky, and H. P. Schadler, Diagonal and off-diagonal quark number susceptibilities at high temperatures, *Phys. Rev. D* **92**, 074043 (2015).
- [8] A. Bazavov *et al.*, The QCD equation of state to  $\mathcal{O}(\mu_B^6)$  from lattice QCD, *Phys. Rev. D* **95**, 054504 (2017).
- [9] A. Bazavov *et al.*, Chiral crossover in QCD at zero and nonzero chemical potentials, *Phys. Lett. B* **795**, 15 (2019).
- [10] Matteo Giordano and Attila Pásztor, Reliable estimation of the radius of convergence in finite density QCD, *Phys. Rev. D* **99**, 114510 (2019).
- [11] A. Bazavov *et al.*, Skewness, kurtosis, and the fifth and sixth order cumulants of net baryon-number distributions from lattice QCD confront high-statistics STAR data, *Phys. Rev. D* **101**, 074502 (2020).
- [12] Philippe de Forcrand and Owe Philipsen, The QCD phase diagram for small densities from imaginary chemical potential, *Nucl. Phys.* **B642**, 290 (2002).
- [13] Massimo D’Elia and Maria Paola Lombardo, Finite density QCD via imaginary chemical potential, *Phys. Rev. D* **67**, 014505 (2003).
- [14] Massimo D’Elia and Francesco Sanfilippo, Thermodynamics of two flavor QCD from imaginary chemical potentials, *Phys. Rev. D* **80**, 014502 (2009).
- [15] Paolo Cea, Leonardo Cosmai, and Alessandro Papa, Critical line of  $2 + 1$  flavor QCD, *Phys. Rev. D* **89**, 074512 (2014).
- [16] Claudio Bonati, Philippe de Forcrand, Massimo D’Elia, Owe Philipsen, and Francesco Sanfilippo, Chiral phase transition in two-flavor QCD from an imaginary chemical potential, *Phys. Rev. D* **90**, 074030 (2014).
- [17] Paolo Cea, Leonardo Cosmai, and Alessandro Papa, Critical line of  $2 + 1$  flavor QCD: Toward the continuum limit, *Phys. Rev. D* **93**, 014507 (2016).
- [18] Claudio Bonati, Massimo D’Elia, Marco Mariti, Michele Mesiti, Francesco Negro, and Francesco Sanfilippo, Curvature of the chiral pseudocritical line in QCD: Continuum extrapolated results, *Phys. Rev. D* **92**, 054503 (2015).
- [19] R. Bellwied, S. Borsányi, Z. Fodor, J. Günther, S. D. Katz, C. Ratti, and K. K. Szabó, The QCD phase diagram from analytic continuation, *Phys. Lett. B* **751**, 559 (2015).
- [20] Massimo D’Elia, Giuseppe Gagliardi, and Francesco Sanfilippo, Higher order quark number fluctuations via imaginary chemical potentials in  $N_f = 2 + 1$  QCD, *Phys. Rev. D* **95**, 094503 (2017).
- [21] J. N. Günther, R. Bellwied, S. Borsányi, Z. Fodor, S. D. Katz, A. Pásztor, C. Ratti, and K. K. Szabó, The QCD equation of state at finite density from analytical continuation, *Nucl. Phys.* **A967**, 720 (2017).
- [22] Paolo Alba *et al.*, Constraining the hadronic spectrum through QCD thermodynamics on the lattice, *Phys. Rev. D* **96**, 034517 (2017).
- [23] Volodymyr Vovchenko, Attila Pásztor, Zoltan Fodor, Sandor D. Katz, and Horst Stoecker, Repulsive baryonic interactions and lattice QCD observables at imaginary chemical potential, *Phys. Lett. B* **775**, 71 (2017).
- [24] Claudio Bonati, Massimo D’Elia, Francesco Negro, Francesco Sanfilippo, and Kevin Zambello, Curvature of

- the pseudocritical line in QCD: Taylor expansion matches analytic continuation, *Phys. Rev. D* **98**, 054510 (2018).
- [25] Szabolcs Borsányi, Zoltán Fodor, Jana N. Günther, Sándor K. Katz, Kálmán K. Szabó, Attila Pásztor, Israel Portillo, and Claudia Ratti, Higher order fluctuations and correlations of conserved charges from lattice QCD, *J. High Energy Phys.* **10** (2018) 205.
- [26] Rene Bellwied, Szabolcs Borsányi, Zoltan Fodor, Jana N. Günther, Jacquelyn Noronha-Hostler, Paolo Parotto, Attila Pásztor, Claudia Ratti, and Jamie M. Stafford, Off-diagonal correlators of conserved charges from lattice QCD and how to relate them to experiment, *Phys. Rev. D* **101**, 034506 (2020).
- [27] Szabolcs Borsányi, Zoltan Fodor, Jana N. Günther, Ruben Kara, Sandor D. Katz, Paolo Parotto, Attila Pásztor, Claudia Ratti, and Kalman K. Szabó, QCD crossover at finite chemical potential from lattice simulations, *Phys. Rev. Lett.* **125**, 052001 (2020).
- [28] Ian M. Barbour, Susan E. Morrison, Elyakum G. Klepfish, John B. Kogut, and Maria-Paola Lombardo, Results on finite density QCD, *Nucl. Phys. B, Proc. Suppl.* **60**, 220 (1998).
- [29] Z. Fodor and S. D. Katz, A new method to study lattice QCD at finite temperature and chemical potential, *Phys. Lett. B* **534**, 87 (2002).
- [30] Z. Fodor and S. D. Katz, Lattice determination of the critical point of QCD at finite T and  $\mu$ , *J. High Energy Phys.* **03** (2002) 014.
- [31] Z. Fodor and S. D. Katz, Critical point of QCD at finite T and  $\mu$ , lattice results for physical quark masses, *J. High Energy Phys.* **04** (2004) 050.
- [32] P. de Forcrand, S. Kim, and T. Takaishi, QCD simulations at small chemical potential, *Nucl. Phys. B, Proc. Suppl.* **119**, 541 (2003).
- [33] Andrei Alexandru, Manfred Faber, Ivan Horváth, and Keh-Fei Liu, Lattice QCD at finite density via a new canonical approach, *Phys. Rev. D* **72**, 114513 (2005).
- [34] Matteo Giordano, Kornel Kapás, Sandor D. Katz, Daniel Nógrádi, and Attila Pásztor, New approach to lattice QCD at finite density; results for the critical end point on coarse lattices, *J. High Energy Phys.* **05** (2020) 088.
- [35] Szabolcs Borsanyi, Zoltan Fodor, Matteo Giordano, Sandor D. Katz, Daniel Nogradi, Attila Pasztor, and Chik Him Wong, Lattice simulations of the QCD chiral transition at real baryon density, *Phys. Rev. D* **105**, L051506 (2022).
- [36] Zoltan Fodor, Sandor D. Katz, and Christian Schmidt, The density of states method at non-zero chemical potential, *J. High Energy Phys.* **03** (2007) 121.
- [37] G. Endrődi, Z. Fodor, S. D. Katz, D. Sexty, K. K. Szabó, and Cs. Török, Applying constrained simulations for low temperature lattice QCD at finite baryon chemical potential, *Phys. Rev. D* **98**, 074508 (2018).
- [38] Szabolcs Borsanyi, Zoltan Fodor, Matteo Giordano, Jana N. Guenther, Sandor D. Katz, Attila Pasztor, and Chik Him Wong, Equation of state of a hot-and-dense quark gluon plasma: Lattice simulations at real  $\mu_B$  vs extrapolations, *Phys. Rev. D* **107**, L091503 (2023).
- [39] Stephen R. Sharpe, Rooted staggered fermions: Good, bad or ugly?, *Proc. Sci. LAT2006* (2006) 022.
- [40] Andreas S. Kronfeld, Lattice gauge theory with staggered fermions: How, where, and why (not), *Proc. Sci. LATTICE2007* (2007) 016.
- [41] A. Bazavov *et al.*, Nonperturbative QCD simulations with 2 + 1 flavors of improved staggered quarks, *Rev. Mod. Phys.* **82**, 1349 (2010).
- [42] Maarten Golterman, Yigal Shamir, and Benjamin Svetitsky, Breakdown of staggered fermions at nonzero chemical potential, *Phys. Rev. D* **74**, 071501 (2006).
- [43] Matteo Giordano, Kornel Kapas, Sandor D. Katz, Daniel Nogradi, and Attila Pasztor, Radius of convergence in lattice QCD at finite  $\mu_B$  with rooted staggered fermions, *Phys. Rev. D* **101**, 074511 (2020); **104**, 119901(E) (2021).
- [44] P. E. Gibbs, The fermion propagator matrix in lattice QCD, *Phys. Lett. B* **172**, 53 (1986).
- [45] Z. Fodor, K. K. Szabo, and B. C. Toth, Hadron spectroscopy from canonical partition functions, *J. High Energy Phys.* **08** (2007) 092.
- [46] Bastian B. Brandt and Gergely Endrodi, Reliability of Taylor expansions in QCD, *Phys. Rev. D* **99**, 014518 (2019).
- [47] D. T. Son and Misha A. Stephanov, QCD at finite isospin density, *Phys. Rev. Lett.* **86**, 592 (2001).
- [48] B. B. Brandt, G. Endrődi, and S. Schmalzbauer, QCD phase diagram for nonzero isospin-asymmetry, *Phys. Rev. D* **97**, 054514 (2018).
- [49] Bastian B. Brandt, Francesca Cuteri, Gergely Endrodi, and Sebastian Schmalzbauer, Exploring the QCD phase diagram via reweighting from isospin chemical potential, *Proc. Sci. LATTICE2019* (2019) 189.
- [50] The Taylor expansion should also diverge in the vicinity of a crossover, due to nearby Lee-Yang zeros in the complex chemical potential plane.
- [51] Sz. Borsanyi *et al.*, Leading hadronic contribution to the muon magnetic moment from lattice QCD, *Nature (London)* **593**, 51 (2021).
- [52] A. Hasenfratz and D. Toussaint, Canonical ensembles and nonzero density quantum chromodynamics, *Nucl. Phys.* **B371**, 539 (1992).
- [53] Stanimire Tomov, Jack Dongarra, and Marc Baboulin, Towards dense linear algebra for hybrid gpu accelerated manycore systems, Technical Report No. 2008-01, 2008.
- [54] J. B. Kogut and D. K. Sinclair, Lattice QCD at finite isospin density at zero and finite temperature, *Phys. Rev. D* **66**, 034505 (2002).
- [55] S. Borsányi, Z. Fodor, J. N. Günther, R. Kara, S. D. Katz, P. Parotto, A. Pásztor, C. Ratti, and K. K. Szabó, Lattice QCD equation of state at finite chemical potential from an alternative expansion scheme, *Phys. Rev. Lett.* **126**, 232001 (2021).
- [56] Szabolcs Borsanyi, Zoltan Fodor, Jana N. Guenther, Ruben Kara, Paolo Parotto, Attila Pasztor, Claudia Ratti, and Kalman K. Szabo, Resummed lattice QCD equation of state at finite baryon density: Strangeness neutrality and beyond, *Phys. Rev. D* **105**, 114504 (2022).
- [57] Colin Morningstar and Mike J. Peardon, Analytic smearing of SU(3) link variables in lattice QCD, *Phys. Rev. D* **69**, 054501 (2004).
- [58] Y. Aoki, G. Endrődi, Z. Fodor, S. D. Katz, and K. K. Szabó, The order of the quantum chromodynamics transition

- predicted by the standard model of particle physics, *Nature (London)* **443**, 675 (2006).
- [59] Szabolcs Borsányi, Zoltan Fodor, Christian Hoelbling, Sandor D. Katz, Stefan Krieg, Claudia Ratti, and Kalman K. Szabó, Is there still any  $T_c$  mystery in lattice QCD? Results with physical masses in the continuum limit III, *J. High Energy Phys.* **09** (2010) 073.
- [60] For the four-flavor theory, it is hard to set the pion mass smaller with staggered fermions, due to the bulk phase discussed in Refs. [61–65].
- [61] Weon-Jong Lee and Stephen R. Sharpe, Partial flavor symmetry restoration for chiral staggered fermions, *Phys. Rev. D* **60**, 114503 (1999).
- [62] C. Aubin and Qing-hai Wang, A possible Aoki phase for staggered fermions, *Phys. Rev. D* **70**, 114504 (2004).
- [63] Anqi Cheng, Anna Hasenfratz, and David Schaich, Novel phase in SU(3) lattice gauge theory with 12 light fermions, *Phys. Rev. D* **85**, 094509 (2012).
- [64] Christopher Aubin, Katrina Colletti, and George Davila, Unphysical phases in staggered chiral perturbation theory, *Phys. Rev. D* **93**, 085009 (2016).
- [65] Andrey Yu. Kotov, Daniel Nogradi, Kalman K. Szabo, and Lorinc Szikszai, More on the flavor dependence of  $m_\rho/f_\pi$ , *J. High Energy Phys.* **07** (2021) 202; **06** (2022) 32.
- [66] Szabolcs Borsanyi *et al.*, High-precision scale setting in lattice QCD, *J. High Energy Phys.* **09** (2012) 010.
- [67] T.D. Lee and Chen-Ning Yang, Statistical theory of equations of state and phase transitions. 2, Lattice gas and Ising model, *Phys. Rev.* **87**, 410 (1952).
- [68] Aydin Deger and Christian Flindt, Determination of universal critical exponents using Lee-Yang theory, *Phys. Rev. Res.* **1**, 023004 (2019).
- [69] Fredrik Brange, Tuomas Pyhäranta, Eppu Heinonen, Kay Brandner, and Christian Flindt, Lee-Yang theory of Bose-Einstein condensation, *Phys. Rev. A* **107**, 033324 (2023).
- [70] Tetsuya Takaishi, Heavy quark potential and effective actions on blocked configurations, *Phys. Rev. D* **54**, 1050 (1996).
- [71] P. de Forcrand, M. Garcia Perez, T. Hashimoto, S. Hioki, H. Matsufuru, O. Miyamura, A. Nakamura, I. O. Stamatescu, T. Takaishi, and T. Umeda, Renormalization group flow of SU(3) lattice gauge theory: Numerical studies in a two coupling space, *Nucl. Phys.* **B577**, 263 (2000).
- [72] Thomas A. DeGrand, Anna Hasenfratz, and Tamas G. Kovacs, Improving the chiral properties of lattice fermions, *Phys. Rev. D* **67**, 054501 (2003).
- [73] Stefano Capitani, Stephan Durr, and Christian Hoelbling, Rationale for UV-filtered clover fermions, *J. High Energy Phys.* **11** (2006) 028.
- [74] Matteo Giordano, Kornel Kapas, Sandor D. Katz, Daniel Nogradi, and Attila Pasztor, Effect of stout smearing on the phase diagram from multiparameter reweighting in lattice QCD, *Phys. Rev. D* **102**, 034503 (2020).
- [75] Luuk H. Karsten, Lattice fermions in Euclidean space-time, *Phys. Lett.* **104B**, 315 (1981).
- [76] Frank Wilczek, On lattice fermions, *Phys. Rev. Lett.* **59**, 2397 (1987).
- [77] Stefano Capitani, Johannes Weber, and Hartmut Wittig, Minimally doubled fermions at one loop, *Phys. Lett. B* **681**, 105 (2009).
- [78] Stefano Capitani, Michael Creutz, Johannes Weber, and Hartmut Wittig, Renormalization of minimally doubled fermions, *J. High Energy Phys.* **09** (2010) 027.
- [79] Stefano Capitani, Michael Creutz, Johannes Weber, and Hartmut Wittig, Minimally doubled fermions and their renormalization, *Proc. Sci. LATTICE2010* (**2010**) 093.
- [80] [www.gauss-centre.eu](http://www.gauss-centre.eu).
- [81] Julich Supercomputing Centre, JUWELS cluster and booster: Exascale pathfinder with modular supercomputing architecture at Juelich Supercomputing Centre, *J. Large-Scale Res. Facil.* **7**, A138 (2021).